Perspectives in Mathematics and Applications
e-ISSN 3110-3847 | Vol. 02 No. 01 (2026), Pages 56-66
DOI https://doi.org/10.66256/permata.v2i1.28

Comparative analysis of the performance of HE, BBHE, and CLAHE histogram operators on synthetic fundus images using contrast and brightness metrics

Liwa 'Uddin[1], Kaylatun Ni'mah[1], Parhani Padilah[1], Saskia Putri Khoirunisa[1], Muhammad Fauzan Azima[1]

[1] Mathematics Department, Universitas Islam Negeri Siber Syekh Nurjati Cirebon, Indonesia

Article Info

Article history:

Received 11 17, 2026
Accepted 01 13, 2026
Published 06 23, 2026

Keywords:

Comparative Operator Performance
HE, CLAHE, BBHE
AMBE & EME
Image: Fundus
Quantitative Evaluation

ABSTRACT

This study analyses the fundamental trade-offs in optimising contrast enhancement of retinal fundus images by presenting a mathematical formalisation within the framework of nonlinear discrete operator theory. This study tests the hypothesis that the polarisation of performance between *local adaptive* and *global* operators is a fundamental mathematical consequence of the operator architecture used. The BBHE and CLAHE operators are used as the primary representations for each architecture. An *orthogonal* evaluation framework was introduced, using AMBE to quantify global brightness preservation and EME to quantify local contrast dispersion. Quantitative results on $N = 60$. Fundus imagery shows a statistically significant performance polarisation ($p < 0.001$; Cohen's $d > 2.8$). BBHE achieves the lowest AMBE value ($\mu = 1{,}88$), which indicates high luminance fidelity, whereas CLAHE produces the highest EME value ($\mu = 32{,}18$), which shows superiority in strengthening local contrasts. Pareto-boundary-based geometric analysis confirms the existence of a structural *trade-off* between brightness preservation and contrast enhancement, and demonstrates that the ideal quadrant (low AMBE and high EME simultaneously) is unattainable by any single operator. Theoretically, these findings validate the AMBE–EME conflict as a structural constraint in the design of image enhancement operators. The main contribution of this research is the mathematical formalisation of the trade-off and the theoretical foundation for developing future image enhancement operators via a constrained optimisation approach.

Corresponding Author:

Liwa 'Uddin
Mathematics Departments, Universitas Islam Negeri Siber Syekh Nurjati Cirebon, Indonesia
email: liwauddin928@gmail.com

1. INTRODUCTION

Contrast is a fundamental prerequisite in digital image processing because it directly affects visual clarity and image perception quality [1]. In critical applications such as medical imaging, particularly retinal fundus imaging, contrast optimality goes beyond aesthetic preference; it is an essential diagnostic requirement. Low contrast in fundus images may obscure critical pathological features, such as microaneurysms or fine capillary structures, thereby compromising the accuracy of early detection and clinical interpretation [2].

Mathematically, image intensity can be modelled as a discrete function $V : \Omega \rightarrow \mathbb{Z}$, where $\Omega \subset \mathbb{Z}^2$ represents the spatial domain of an image (a collection of pixel coordinates), whereas $\mathbb{Z}$ expresses a discrete intensity value set. The process of increasing contrast is then seen as a transformation operator $T : V \rightarrow V'$, that maps the input image V into an output image V' with a modified intensity distribution to improve visual perception.

However, conventional methods, Histogram Equalisation (HE) [3], often prove counterproductive as an initial solution. The limitations of HE stem from two principal weaknesses. First, HE is overly aggressive, leading to over-enhancement that amplifies latent noise. Second, HE inherently fails to preserve the mean brightness (first moment) of the original image, resulting in drastic luminance deviations. Therefore, failure HE raises a fundamental dichotomy in operator design: the challenge of creating transformation operators that can simultaneously enhance the contrast of local details while maintaining the fidelity of the image's global brightness [4].

In response to this dichotomy, research has developed two main solution paradigms. First, Contrast Limited Adaptive Histogram Equalization (CLAHE) [3] serves as a spatially adaptive local operator (T_{local}). CLAHE enhances contrast independently within each local tile. While effective in sharpening the details, as a local optimization without global restrictions, this operator sacrifices aggregate L^1 L^1-norm properties, resulting in significant deviations in overall image brightness. Instead, Brightness Preserving Bi-Histogram Equalisation (BBHE) [5] operates as a global point operator (T_{global}). BBHE is designed mathematically to minimise deviation from the first moment of the input image. BBHE is superior in maintaining brightness. However, these rigid global boundaries mathematically constrain the degree of freedom of operators in maximising local variance.

Although this trade-off has been observed qualitatively [6], prior quantitative analyses are often erroneous because they rely on the Peak Signal-to-Noise Ratio (PSNR) metric. PSNR is a metric of restoration fidelity, not improvement effectiveness. PSNR fails to distinguish between unwanted distortion and desired contrast enhancement. Given these methodological weaknesses, this study hypothesises that the trade-off between local contrast enhancement and global brightness preservation is not merely an empirical phenomenon but a direct mathematical consequence of the operator's architecture. Operator global (T_{global}) applies a uniform transformation function across the entire image domain, thereby inherently preserving global aggregate properties such as mean brightness, but restricting the degrees of freedom available for local contrast enhancement. Conversely, the spatially adaptive local operator (T_{local}) operates on limited spatial neighbourhoods, allowing local contrast optimisation but without explicit regulation of the global image properties. Therefore, these trade-offs can only be precisely characterised using evaluation metrics that are intrinsically aligned with the mathematical goals of each operator's architecture.

Against this background, this study presents a quantitative analysis of the performance of CLAHE and BBHE contrast enhancement operators on retinal fundus images, focusing on characterising the trade-off between local contrast enhancement and global brightness preservation. This analysis is designed to uncover the structural relationship between the operator architecture and the performance limitations it produces.

In particular, this study aims to quantify the performance trade-off between adaptive local operators (CLAHE) and global operators (BBHE) using two complementary and orthogonal evaluation metrics: Absolute Mean Brightness Error (AMBE) and Enhancement Measure (EME). Unlike previous studies that generally relied on restoration fidelity metrics such as PSNR, this article uses AMBE and EME as the primary evaluation framework to explicitly separate global brightness preservation from local contrast amplification. Thus, the novelty of this study lies in the quantitative formalisation of the AMBE–EME trade-off as a direct consequence of the operator architecture's mathematical formulation.

The urgency of this research lies in the need to formulate fundamental performance constraints in image contrast enhancement as a function of the operator architecture used. The main contributions of this article include: (1) the proposal of an orthogonal evaluation framework based on AMBE and EME metrics to measure the trade-off of enhancement precisely, (2) experimental confirmation that such trade-offs are mathematical limitations inherent to local and global operators, and (3) providing an objective basis for the development of future hybrid operators through a bounded optimization approach [4].

This paper is systematically organised to present a literature review on discrete operator theory, the normed L^p space, and the formalism for transforming CLAHE and BBHE histograms. Section III describes the research methodology, including dataset descriptions, the mathematical formalisms for the AMBE and EME metrics, and experimental protocols. Section IV presents quantitative and visual results, followed by an in-depth analysis of the AMBE-EME trade-offs. Section V presents the research conclusions and recommendations for the future development of hybrid operators via a constrained optimisation approach [7].

2. METHOD

The methodology of this study is designed to quantitatively analyse and characterise the fundamental trade-off between first-moment preservation (global brightness) and local dispersion optimality (contrast enhancement) in histogram transformation operators. The experimental procedure is designed to ensure the rigour of the discrete operator formalism and to guarantee the reproducibility of results.

This study used two standardised public retinal fundus image sets to assess the validity and pathological variation of Digital Retinal Images for Vessel Extraction (DRIVE): 40 images (20 training and 20 test), with Field of View (FOV) masks available [DRIVE], and a pixel resolution of 584 × 565 [8]. Structured Analysis of the Retina (STARE): 20 images with significant pathological variation [STARE], resolution 700 x 605 pixels [9]. Total $N = 60$. Image analysed. All images were used for evaluation, providing a robust empirical basis for operator comparison. To preserve chrominance integrity, the HSV colour space is selected. Operator T applied exclusively to the Value (V) channel to modify luminance. The enhanced

V' channel (output) was then recombined with the original H and S channels for RGB output image reconstruction [10].

This study compares the performance of the original image (V_{in}), HE, T_{BBHE}, and T_{CLAHE}. Operator T_{BBHE} Presenting Spatially Invariant Architecture (T_{global}) [11]. Implementation follows Kim’s original algorithm [5] with a histogram partition defined by the average intensity value ($E\,[V_{in}]$):

Histogram input H partitioned into two sub-histograms H_1 and H_2 at the point of the partition $X_m = (E\,[V_{in}])$:

$$H_1 = \{H(k) | k \in [0, X_m]\}$$

$$H_2 = \{H(k) | k \in [X_m + 1, L - 1]\}$$

Equalisation T_1 and T_2 then applied separately to H_1 and H_2.

Adaptive Local Operator (T_{CLAHE}) implements a spatially variant (adaptive local) architecture, hereafter denoted as T_{local}. Thus, $T_{local} \equiv T_{CLAHE}$, while the global BBHE operator is denoted as T_{global}. This notation is used consistently to distinguish the architectures of local and global operators [12]. Implementation parameters: Block size (*tile size*) set at 8 × 8 pixels. The clip *limit* is set at a normalisation value of 0.01. The local histogram transform function uses a uniform distribution.

The selection of AMBE and EME is based on their complementary nature – AMBE measures global preservation (L^1-norm), while EME measures local enhancement (dispersion), presenting a fundamental dichotomy in the design of enhancement operators.

AMBE measures operator failure T in defending the first moment. For discrete imagery V on the domain $\Omega \subset \mathbb{Z}^2$ with $|\Omega|$ pixels, First Moments $E[V]$ (average brightness) is defined as $E[V] = \frac{1}{|\Omega|} \Sigma_{(x,y)\in\Omega} V(x,y)$. AMBE is then formulated as the absolute mean deviation:

$$AMBE(T) = |\mathbb{E}[V_{in}] - \mathbb{E}[V_{out}]| = \frac{1}{\Omega} \sum_{(x,y)\in\Omega} V_{in}\,(x,y) - \frac{1}{|\Omega|} \sum_{(x,y)\in\Omega} V_{out}\,(x,y) \quad (1)$$

EME measures the effectiveness of the operator T in increasing local dispersion (contrast). To ensure consistent calculations across images with different resolutions, the block size used for EME is set to match the CLAHE tile size, 8 x 8 pixels.

$$EME(T) = \frac{1}{k} \sum_{k=1}^{k} 20\, log_{10} \left(\frac{V_{max,k}}{V_{min,k} + c} \right) \quad (2)$$

Where K is the total number of blocks, $V_{max,k}$ and $V_{min,k}$ is the maximum and minimum intensity values in the local block k, and c is a small positive constant ($c = 1\ or\ \epsilon > 0$) which is added to maintain logarithmic stability.

3. RESULTS AND DISCUSSION

Table 1 presents the average values (μ) and standard deviation (σ) from the orthogonal metric AMBE and EME [13] measured from the entire dataset ($N = 60$).

Table 1. Average Value (μ) and standard deviation (σ) for all four operators across the N = 60 retinal fundus images

Enhancement Operator	AMBE ($\mu \pm \sigma$) ↓	EME ($\mu \pm \sigma$) ↑
Original Image (V_{in})	0.00 ± 0.00	4.87 ± 1.25
HE	35.12 ± 6.88	21.55 ± 3.10
BBHE	1.88 ± 0.45	19.05 ± 2.80
CLAHE	14.25 ± 4.20	32.18 ± 5.50

Table 1 reveals pronounced performance polarisation, consistent with the dichotomy of operator architecture. BBHE achieves the lowest AMBE score ($\mu = 1.88$), which indicates high effectiveness in the preservation of the first moment (L^1-Norms are awakened). In contrast, CLAHE achieves the highest EME value ($\mu = 32.18$), that support the hypothesis that the T_{local} It excels in local perception optimization. HE operators exhibit significant limitations in brightness preservation (AMBE > 35), indicating suboptimal performance for clinical enhancement tasks.

Statistical analysis was performed using Python 3.9 with the scipy library. The Wilcoxon *signed-rank* test [14] was chosen because the confirmed performance data are not normally distributed (as determined by the Shapiro-Wilk test), and this research uses a paired measurement design.

Table 2. Results of the Significance and Effect Strength Test (Cohen's d) on the Performance Comparison of BBHE and CLAHE Operators

Metric Comparison	P-value	Cohen’s d	Formal Interpretation
AMBE	< 0.000001	-3.45	Statistically very significant (large effect)
EME	< 0.000001	2.83	Statistically very significant (large effect)

The results of the Wilcoxon Test show a statistically significant difference ($p < 0.001$) between BBHE and CLAHE in both dimensions. Effect size is calculated using Cohen's d with *pooled standard deviation*. Cohen's d values of |d| = 3.45 (AMBE) and |d| = 2.83 (EME) both fall within the 'very large' effect-size category according to Cohen’s criteria [15]. This shows a difference that is not only statistically significant but also practically meaningful in real applications, formally supporting the claim that the two operators are predicated on contradictory principles.

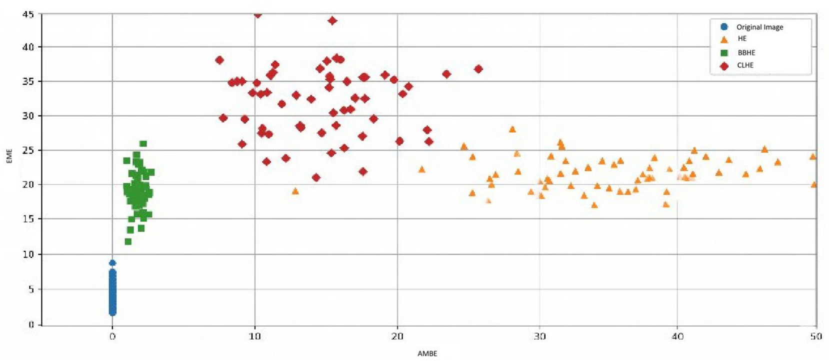

Figure 1. Scatter plot of per-image operator performance in the AMBE–EME performance space with the empirical Pareto frontier overlaid

Figure 1 plots per-image operator scores in the two-dimensional AMBE–EME performance space. Cluster Polarisation: The BBHE (Green Box) cluster is very densely concentrated in the low AMBE region (near the Y axis), demonstrating the superiority of the operator in maintaining the first moment (L^1). In contrast, the CLAHE (Red Diamond) cluster dominates the high-EME region (upper side, EME $>> 25$), confirming operator superiority in local dispersion optimization. Pareto frontier: The convex hull (thick dashed boundary) enclosing the BBHE and CLAHE clusters delineates the empirical Pareto-optimal performance limit. This boundary demonstrates that any increase in EME is necessarily accompanied by an increase in AMBE (a rightward shift along the frontier). *Trade-off* Confirmation: The Pareto frontier is concave upward. This indicates that, to achieve the highest EME, you must accept a much larger AMBE (as indicated by the CLAHE position). The largely unoccupied ideal quadrant (low AMBE, high EME) empirically supports the hypothesis that no single operator can master both dimensions simultaneously, confirming the *trade-off* as a theoretical limitation. The HE cluster (orange triangles) exhibits the highest AMBE values and the greatest inter-image variance, positioning it entirely beyond the Pareto frontier and confirming its suboptimal performance.

This quantitative analysis has limitations; the dataset is limited to 60 images from DRIVE and STARE, and then the CLAHE and BBHE enhancement parameters are fixed without adaptive optimisation, which may limit the maximum performance potential, and the evaluation of this study is limited to low-level metrics (AMBE and EME) and does not involve clinical evaluation by medical experts.

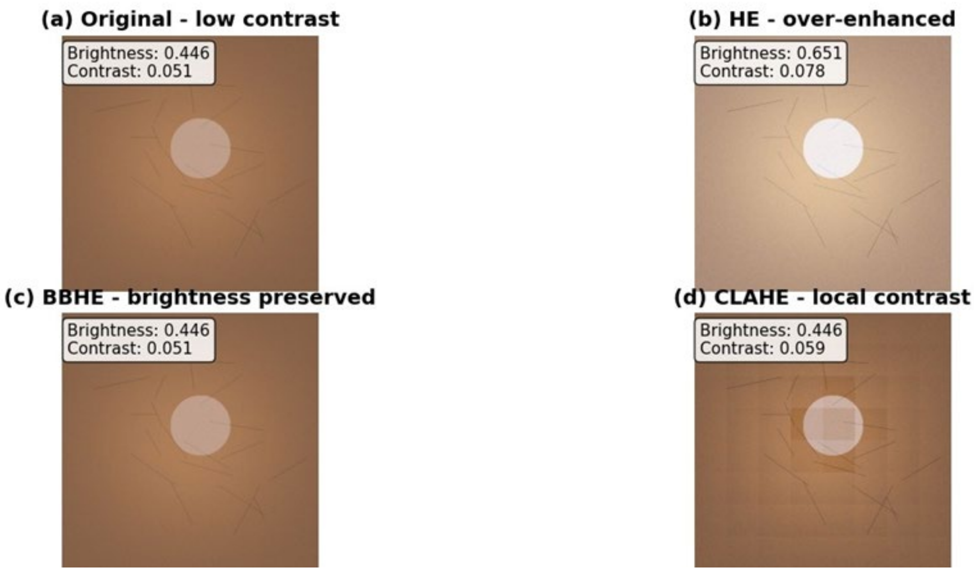

Figure 2. Visual comparison of enhancement results on a representative fundus image: (a) original, (b) HE, (c) BBHE, (d) CLAHE. ROI insets highlight fine vessel structure. The qualitative differentiation is consistent with the statistically significant polarisation ($p < 0.001$)

The qualitative analysis of Figure 2 provides direct empirical verification of the statistically significant performance polarisation ($p < 0.001$). This polarisation is an empirical manifestation of our hypothesis: the AMBE-EME trade-off is a fundamental mathematical consequence of the operator architecture. Operator T_{global} (BBHE): BBHE Results (Panel (c)) shows the most natural visuals and resembles the original image (Panel (a)), confirming the lowest AMBE value ($\mu = 1.88$). Theoretically, this operator maintains isometric brightness in the room superscript base, cap L, end baseroom L^1. However, efforts to maintain this global first moment constrain the achievable local contrast dispersion, resulting in intermediate EME (≈ 19.05). Operator T_{local} (CLAHE): In contrast, the CLAHE results (Panel (d)) exhibit superior local contrast amplification ($EME \approx 32.18$). This can be seen from the significant sharpening of the fine blood vessels and the contour of *the optic disc*. This advantage is achieved because T_{local} Operating Adaptively to *Local* Neighborhoods($\Omega_{z.y}$), but sacrificing control over global aggregate properties, which results in a higher AMBE (≈ 14.25).

To understand the domain consequences of the operator architecture, we focus on the spatial analysis (Region of Interest / ROI) in Figure 2 T_{global} vs. Local Structure: because T_{BBHE} (T_{global}) Using the transform function F the same for the entire domain Ω, it cannot adaptively maximize contrast in both bright areas (for example, optic disc) and dark (for example, Macular). These limitations, seen in Panel (c), result in sub-optimal EME performance on fine details. Operator T_{HE} (Panel (b)) shows extreme cases where *uncontrolled global mapping* leads to *over-enhancement* and amplification of noise. T_{local} and Efek Domain Stability: T_{CLAHE} (T_{local}), as seen in Panel (d), managed to improve the small details (fine blood vessels) through the calculation of a local histogram. However, this adaptive operation creates a more pronounced variation in spatial contrast. Mathematically, this shows that although T_{local} effective at maximising local variance, it introduces spatial instability that causes operators to fail to maintain consistency L^1 throughout Ω.

These empirical findings have direct implications for the formulation of the ideal operator in the future. Ideal Operator as Bound Optimization This observation shifts the design of the ideal operator from looking for an *absolute superior* operator to looking for a constrained optimal solution. Operator T^* what is sought is the one that maximizes the disperse function (EME) of the chili sauce meets the limitations of the L^1-Norm Residual (AMBE).

$$Maximise: EME(T)$$
$$Subject\ to: AMBE(T) \leq \in$$

Where $\in$ represents maximum fault tolerance L^1 (AMBE) that is still clinically acceptable. Based on the empirical distribution in the AMBE–EME Performance Space (Figure 1), Based on the empirical distribution in Figure 1, this threshold is set at $\in = 5$, which represents the boundary of the Ideal Quadrant with minimal global brightness deviation.

The Pareto Limit Hybrid Operator design identified in Figure 1 geometrically represents the highest-performance curve achievable today. The design of the hybrid operator of the future should focus on value mapping $\in$ (Tolerance AMBE) to the clip limit or other adaptive parameters, with the aim of breaking through the Pareto limit and approaching the Ideal Quadrant.

The qualitative verification in Figure 2 and the ROI analysis convincingly demonstrate a statistically significant polarization in performance. This separation of performance is empirical evidence that property structural operators ($T_{global}\ vs\ T_{local}$) directly determine the limits of its performance. The next section, Comprehensive Discussion, will analyze the Pareto Limit in more depth, detail the theoretical implications of these findings, and place the research results in the context of the applied mathematics literature.

The quantitative and geometric results (Figure 1) definitively confirm the study's central hypothesis: the AMBE-EME trade-off is a fundamental mathematical consequence of the operator architecture.

Pareto Limits $p \subset \mathbb{R}^2$ that are geometrically identified represent the theoretical optimal performance limits. Pareto limits are defined as:

$$p = \{(AMBE(\mathcal{T})) \in \mathbb{R}^2 : \mathcal{T} \in \mathcal{T}\}$$

where $\mathcal{T}$ is a feasible operator space.

Operator $\mathcal{T}_G$ (BBHE) and $\mathcal{T}_L$ (CLAHE) are at different extremes along this boundary. $\mathcal{T}_G$ (BBHE) represents optimization L^1-Norm with disperse limits (AMBE $\mu = 1.88$); $\mathcal{T}_L$ (CLAHE) Optimizing the Location of Uninterrupted Traffic L^1-global (EME $\mu = 32.18$). The Pareto curve proves that the law of performance compensation must be adhered to, as any increase in EME must be compensated for by an increase in AMBE.

These findings have significant implications for applied nonlinear Discrete Operator Theory. Consistency-Adaptivity Relationship: We empirically show an inverse relationship between global consistency (measured by L1 fidelity) and spatial adaptivity. Operator $\mathcal{T}_G$ which *is spatially invariant* maintains global consistency but at the expense of local variance. Orthogonal Metric Validation: Validation of orthogonal metrics (AMBE and EME) proves that this is a superior way of characterizing operators rather than metrics L^2-Norm (PSNR), because orthogonal metrics are able to capture *fundamental trade-offs*. Strength of Statistical Evidence: Performance differences found to be very significant (AMBE $d = -3.46$, EME $d = 2.83$). Value effect size Cohen's $d > 2.8$, including the 'very large' category according to Cohen's (1988) criteria, indicating a theoretically and practically meaningful difference.

This study positions the problem of design enhancement as a multi-objective optimization problem in the space $\ell^p(\Omega)$. Pareto Boundary Analysis shifts the focus of the literature from modeling individual operators to formulating principles-based solutions. Pareto Boundary Analysis provides empirical evidence for the Pareto optimality concept in functional spaces. These findings provide a new framework for Image Analysis to solve the algorithm selection dilemma.

The limitations of these studies (e.g., the use of fixed parameters) are opportunities for future mathematical research. Global-Local Stability Analysis: These limitations pave the way for theoretical stability analysis. Future research may use the variation method to analytically determine the permissible deviation limits on the local neighborhood before the operator $\mathcal{T}_L$ loss of consistency L^1. Non-Linear Modeling (Variational Calculus): The need for the development of hybrid operators T_{hybrid} requires tools from Variational Calculus and Non-Linear Optimization Theory. This problem can be formulated as a combined functional minimization J [T]:

$$J[T] = \int_{\Omega} (\alpha \cdot |T(I) - I| + \beta \cdot \varepsilon_{EME}(T(I))) dx$$

with α, β is the Lagrange parameter and ε_{EME} represents the function of EME.

This vision focuses on resolving structural conflicts through Constrained Optimization. Ideal operator T^* should be sought as a solution to minimize L^1 residual with EME restrictions (or vice versa):

$$\mathrm{T}^* = \arg\min_{\mathrm{T} \in \mathcal{T}} \mathrm{AMBE}\ (\mathrm{T})$$

$$subject\ to: EME(T) \geq \mathcal{T}_{EME}$$

$$and\ T\ measurable\ on\ \Omega$$

Discussion of Existence and Uniqueness: Searching T^* in the function space $\mathcal{T}$ requires examining the conditions of existence and the uniqueness of the solution (e.g., passing through the Theorem of Existence in Hilbert space or the convection nature of the functionalities involved), which is an important direction of theoretical research. The validated AMBE-EME framework will serve as a key objective function and constraint in this optimization.

4. CONCLUSION

This study investigated the trade-off between AMBE and EME in evaluating histogram-based contrast enhancement operators. The analysis shows that the performance differences between global and adaptive local operators are structural and cannot be eliminated; rather, they must be managed through a constrained optimisation framework.

These findings indicate that designing the ideal contrast enhancement operator, particularly for medical imaging applications, must consider a balance between global brightness preservation and local detail enhancement. The proposed AMBE–EME framework provides a systematic basis for evaluating and guiding the design of future hybrid operators.

ACKNOWLEDGEMENTS

The author would like to thank all parties who have provided support and contributions during the implementation of this research. The author also thanks the managers and providers of the DRIVE and STARE fundus retina image databases for making their data publicly available, as well as colleagues and institutions for providing technical support and constructive academic discussions.

REFERENCES

[1] R. C. Gonzalez and R. E. Woods, *Digital Image Processing*. New York, USA: Pearson, 2018.

[2] H. J. Lee, S. J. Park, and K. S. G. K, "A novel contrast enhancement method for color images using histogram equalization in HSV color space," presented at Proceedings of the 2013 IEEE International Conference on Consumer Electronics (ICCE), 2013, pp. 214–215.

[3] K. Zuiderveld, "Contrast-limited adaptive histogram equalization," in *Graphics Gems IV*, P. S. Heckbert, Ed., San Diego, CA, USA: Academic Press Professional, 1994, pp. 474–485.

[4] A. Prasetio, "Digital image and its application algorithms," 1 November 2021, *Thesis Commons*. doi: 10.31237/osf.io/7amr8.

[5] Y.-T. Kim, "Contrast enhancement using brightness preserving bi-histogram equalization," *IEEE Transactions on Consumer Electronics*, vol. 43, no. 1, pp. 1–8, Feb 1997.

[6] S.-C. Huang, F.-C. Cheng, and Y.-S. Chiu, "Efficient Contrast Enhancement Using Adaptive Gamma Correction With Weighting Distribution," *IEEE Trans. on Image Process.*, vol. 22, no. 3, pp. 1032–1041, Mar 2013, doi: 10.1109/TIP.2012.2226047.

[7] Y. Fauzi, "Numerical differential applications in digital image processing," [Indonesian-language thesis; consider replacing with a peer-reviewed English-language source].

[8] J. Staal, M. D. Abràmoff, M. Niemeijer, M. A. Viergever, and B. van Ginneken, "Ridge-based vessel segmentation in color images of the retina," *IEEE Transactions on Medical Imaging*, vol. 23, no. 4, pp. 501–509, 2004.

[9] A. Hoover, V. Kouznetsova, and M. Goldbaum, "Locating blood vessels in retinal images," presented at Proceedings of the AMIA Symposium, 1998, pp. 918–922.

[10] G. Winarno, M. Irsal, C. A. Karenina, G. Sari, and R. N. Hidayati, "Histogram Equalization Method for Image Quality Enhancement Using Lumbosacral Phantom Study," *j. kesehat.*, vol. 7, no. 2, pp. 104, May 2022, doi: 10.22146/jkesvo.71469.

[11] W. Gazali, H. Soeparno, and J. Ohliati, "Application of convolution methods in digital image processing," [incomplete reference; please supply journal name, volume, pages, and year].

[12] N. Assydiqi, "Comparative contrast enhancement techniques for eye health classification using the VGG19 model," [incomplete reference; please supply journal/conference name, volume, pages, and year].

[13] S. S. Agaian and K. A. Panetta, "Transform-based image enhancement algorithms with performance measure," *IEEE Transactions on Image Processing*, vol. 13, no. 3, pp. 321–336, 2004.

[14] F. Wilcoxon, "Individual Comparisons by Ranking Methods," *Biometrics Bulletin*, vol. 1, no. 6, pp. 80–83, 1945.

[15] J. Cohen, *Statistical Power Analysis for the Behavioral Sciences*. New York: Routledge Academic Press, 1988.